ORIGINAL PAPER

Terrestrial versus aquatic source identification of sedimentary *n*-alkane and sugar biomarkers: a case study from the Bale Mountains, Ethiopia

Betelhem Mekonnen · Lucas Bittner · Tobias Bromm · Bruk Lemma · Bruno Glaser · Wolfgang Zech · Sileshi Nemomissa · Tamrat Bekele · Michael Zech

Abstract Organic matter in sedimentary archives is abundantly used to reconstruct paleoenvironmental and climate histories. Thereby, distinguishing between the terrestrial and aquatic origin of sedimentary organic matter is often a prerequisite for robust interpretations. In this case study, we use published data for modern plants and topsoils to identify the terrestrial versus aquatic source of *n*-alkane and sugar biomarkers in two afro-alpine sediment archives (Lake Garba Guracha and Depression B4) in the Bale Mountains, Ethiopia. The results of our comparative approach show that the long-chain *n*-alkanes C_{29}, C_{31}, and C_{33} in the sedimentary archives yielded patterns similar to those typical for the potential terrestrial input. By contrast, the relative abundances of the sedimentary mid-chain *n*-alkanes C_{23} and C_{25}, and at least partly C_{27}, are significantly increased compared to the plants and topsoils. This suggests that they are primarily produced by aquatic macrophytes and microorganisms. The P_{aq} ratio $(C_{23} + C_{25})/(C_{23} + C_{25} + C_{29} + C_{31})$ is validated as a suitable source identification proxy in our study area. The sugar biomarkers xylose (xyl) and arabinose (ara) are abundant in the plant and topsoil samples. By comparison, high relative abundances of fucose (fuc) and rhamnose (rham) are generally only observed in sediments. This indicates

B. Mekonnen (✉) · T. Bromm · B. Lemma · B. Glaser
Institute of Agricultural and Nutritional Sciences, Soil Biogeochemistry, Martin Luther University Halle-Wittenberg, Wittenberg, Germany
e-mail: betymekonnen19@gmail.com

T. Bromm
e-mail: tobias.bromm@landw.uni-halle.de

B. Lemma
e-mail: bruk_lemma@yahoo.com

B. Glaser
e-mail: bruno.glaser@landw.uni-halle.de

L. Bittner · M. Zech
Chair of Physical Geography with focus
on paleoenvironmental research, Technische Universität Dresden, Dresden, Germany
e-mail: lucas.bittner@tu-dresden.de

M. Zech
e-mail: michael.zech@tu-dresden.de

B. Lemma
Forest and Rangeland Biodiversity Directorate, Ethiopian Biodiversity Institute, Addis Ababa, Ethiopia

W. Zech
Department of Soil Science, University of Bayreuth, Bayreuth, Germany
e-mail: w.zech@uni-bayreuth.de

S. Nemomissa · T. Bekele
Department of Plant Biology and Biodiversity Management, Addis Ababa University, Addis Ababa, Ethiopia
e-mail: sileshi.nemomissa@aau.edu.et

T. Bekele
e-mail: tambek07@gmail.com

that these sugar biomarkers are primarily produced by aquatic macrophytes or micro-organisms. Therefore, the ratio (fuc + rham)/(ara + xyl) is a suitable sugar biomarker proxy for organic matter source identification. The relative abundances of galactose and mannose are systematically decreasing and increasing, respectively, from leaves over O-layers to Ah-horizons. Furthermore, they are not significantly different from the abundances found in the sediments. This hinders terrestrial versus aquatic source identification using galactose and mannose.

Keywords Organic matter source

Introduction

Sedimentary organic matter in lake sediments is frequently used for paleoenvironmental and climate studies (Meyers and Ishiwatari 1993; Smol et al. 2002). Organic matter originates from the complex mixture of lipids, carbohydrates, proteins, and other components produced by organisms that have lived in (autochthonous) and around the lake (allochthonous) (Smol et al. 2002). As a result, organic matter source identification is an essential prerequisite for robust paleoenvironmental reconstructions (Doyle et al. 2022). During the last decades, different molecular markers and proxies were therefore suggested and developed for characterizing the organic matter and its degree of alteration in sedimentary records (Meyers and Ishiwatari 1993; Meyers 1994; Andersson et al. 2012). For instance, the total organic carbon to nitrogen ratio (TOC/TN) is used to distinguish between terrestrial and aquatic carbon sources. Organic matter derived from algae shows low TOC/TN values (between 4 and 10), whereas vascular land plants are usually characterized by high TOC/TN values (≥ 20) (Meyers 1994). Similarly, the stable carbon isotopic composition $\delta^{13}C$ is frequently used to distinguish between C3 and C4 plant-derived organic matter (Meyers and Ishiwatari 1993; Meyers and Lallier-Vergès 1999). However, TOC/TN and $\delta^{13}C$ values are affected by mineralization and degradation, resulting in more positive $\delta^{13}C$ values and a lower TOC/TN ratio (Meyers 1994). Moreover, the Hydrogen and Oxygen Indexes, which represent the amount of hydrogen and oxygen in organic matter, may be used as proxies for organic matter source identification

(Talbot and Livingstone 1989; Lüniger and Schwark 2002). Note that both indexes are affected by degradation, too.

In addition to the bulk parameters introduced above, molecular biomarkers such as *n*-alkanes (Ficken et al. 2000; Doyle et al. 2022) and hemicellulose-derived neutral sugars (Hepp et al. 2016) have been suggested for organic matter source identification. This is based on different biomarker patterns in vascular plants versus aquatic organisms. For instance, long-chain *n*-alkanes are abundant components of most vascular plant epicuticular waxes (Eglinton and Hamilton 1967; Bush and McInerney 2013), while mid- and short-chain *n*-alkanes predominate in many aquatic macrophytes and algae, respectively (Ficken et al. 2000, 2002). Similarly, the applicability of sugar biomarkers in paleoenvironmental studies is based on the notion that polysaccharides synthesized by vascular plants contain high amounts of pentose sugars (arabinose and xylose), whereas those synthesized by micro-organisms are dominated by hexose sugars (galactose, mannose, rhamnose, and fucose) (Oades 1984; Cheshire 1979).

The Bale Mountains in the southeast highland of Ethiopia comprise Africa's largest afro-alpine area, the Sanetti Plateau, above 4000 m asl (Hillman 1988; Miehe and Miehe 1994). Numerous small lakes and depressions make this area favourable for paleoenvironmental reconstructions. Even though they are few in number, paleoenvironmental and anthropological studies of the Bale Mountains (Wesche et al. 2000; Umer et al. 2007; Tiercelin et al. 2008; Kuzmicheva et al. 2014; Gil-Romera et al. 2019; Ossendorf et al. 2019; Groos et al. 2021) reveal major climatic events, vegetation changes, and anthropogenic influence. Therefore, in-depth studies of sedimentary archives can provide substantial knowledge on the past and future effects of climate change and anthropogenic activities at local and regional scales.

This study aims to identify the sources of *n*-alkane and sugar biomarkers in two sedimentary archives located at high altitudes in the Bale Mountains, namely the glacial cirque lake Garba Guracha and a depression called B4 located on the Sanetti Plateau. Bittner et al. (2020) presented the Paq ratio and sugar proxy (fuc + xyl)/ara for Garba Guracha sediments previously and Mekonnen et al. (2022) provided the Paq ratio for B4 depression sediments. However, a systematic comparison of the whole datasets with

regional reference plants and soils has not been carried out hitherto. Therefore, for this systematic comparison, we use published data from Lemma et al. (2019) and Mekonnen et al. (2019), who previously chemotaxonomically characterized modern plants and soils along the southwest and northeast transects of the Bale Mountains using *n*-alkane and sugar biomarkers, respectively.

Study site

The Bale Mountains belong to the Bale-Arsi Massif, located east of the Main Ethiopian Rift in the Oromia Regional State, southeast of Ethiopia, between 6.4833333°–7.1666667° N and 39.5°–39.9666667° E (Fig. 1). The Bale Mountains National Park covers an area of ~2200 km^2, including the most extensive continuous high-altitude afro-alpine plateau, the Sanetti Plateau, and the peak, Tullu Dimtu, at 4377 m asl (Kidane et al. 2012). The mountains rise from the eastern highlands beside the Ethiopian Rift Valley from 2500 m asl to the Sanetti Plateau at 3800–4000 m asl (Hillman 1988). The geology of the Bale Mountains is characterized by volcanic material consisting of alkali basalt, trachyte, and tuffs with rhyolites formed during the Miocene and Oligocene (Billi 2015). Studies indicate that high altitudes of the mountains (>3000 m asl) were glaciated during the Last Glacial Maximum (Osmaston et al. 2005). The soils of the Bale Mountains are generally shallow and rich in stones. They are made of silty loam that ranges from reddish brown to black. Andosols, Leptosols, and Cambisols are common types of soils in the Bale Mountains. Moreover, muddy Gleysols are found in wetlands and sedimentary basins (Yimer 2007).

Due to the differences in elevation and aspect, the climate of the Bale Mountains varies from north to south (Kidane et al. 2012). The mean annual temperature is 11.8 °C at Dinsho (the Bale Mountains National Park headquarters at 3170 m asl), while the mean minimum temperature is around 0.6 °C in mountainous areas (Hillman 1988; Miehe and Miehe 1994). The precipitation of the Bale Mountains is governed by the movement of the Intertropical Convergence Zone and Congo Air Boundary, resulting in longer rainy (March–October) and shorter dry (November–February) seasons. The rainy season is bimodal, with a maximum from July to October and a second peak from
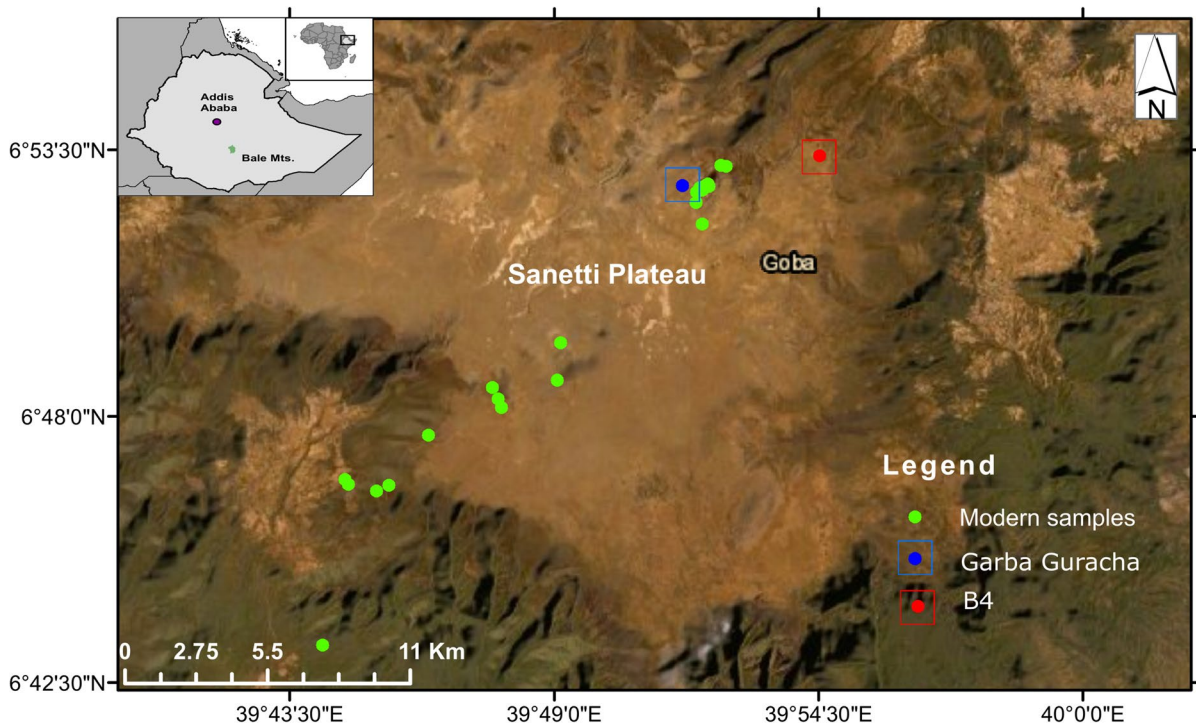

Fig. 1 Map showing the geographical location of the study area and sampling sites

March to June. While the northeasterly winds from the Arabian Peninsula dominate during the dry season, the southwesterly monsoon transports moisture from the Indian Ocean and the Atlantic Ocean via the Congo Basin during the rainy seasons (Tierney et al. 2013; Lemma et al. 2020). The southwestern part of the Bale Mountains experiences the highest precipitation and humidity, with 1000–1500 mm/yr, and the northern part receives annual rainfall ranging between 800 and 1000 mm/yr (Woldu et al. 1989). The Sanetti Plateau is characterized by strong diurnal temperature fluctuations and night frost (Hillman 1988).

Following the climate variability along altitude, the vegetation of the Bale Mountains is divided into three main zones: the afromontane, the Ericaceous, and the afro-alpine belt (Hedberg 1951; Friis 1986). The afromontane forest, which is further divided into dry and moist afromontane forests, covers an altitude of 1450–3750 m asl. The dry afromontane forest in the north is dominated by *Juniperus procera, Hagenia abyssinica*, and *Hypericum revolutum* (Yineger et al. 2008), while the southern afromontane forest is dominated by *Warburgia ugandensis, Croton macrostachyus, Podocarpus falcatus*. The Ericaceous belt spans between 3200 and 3800 m asl and is characterized by *Erica arborea* and *Erica trimera* in the form of shrubland in most parts and moist forest on the southern slopes (Harenna forest). Finally, the afro-alpine vegetation is characterized by *Helichrysum splendidum-Alchemilla haumannii* dwarf-scrubs, *Kniphofia foliosa* Giant *Lobelia* (*L. rhynchopetalum*) and grasses (Hedberg 1964), accompanied by patches of *Erica* growing beside big boulders above 3800 m asl. The wetlands of the Bale Mountains at higher altitudes are mainly characterized by wetland plant species such as *Carex monostachya, Haplocarpha rueppellii, Ranunculus* sp. and *Eriocaulon schimperi* (Dullo et al. 2015; Chignell et al. 2019). Water plants such as *Potamogeton thunbergii* and *Ranunculus trichophyllus* and *Pediastrum* algae are common on the shallow lakes nearby the B4 depression (Mekonnen et al. 2022).

Materials and methods

Sample collection

Modern reference samples (leaves as well as surface soil samples from O-layers and Ah-horizons) were collected from the northeastern and southwestern transects (3870 to 4134 m asl and 2550 to 4377 m asl,

respectively) of the Bale Mountains, including the surrounding area of Garba Guracha (Fig. 1). Twenty-five leaf samples from *Erica* spp. and afro-alpine plants such as *Alchemilla haumannii, Helichrysum splendidum, Lobelia rhynchopetalum, Kniphofia foliosa*, and *Festuca abyssinica*, and 38 surface soil samples (15 humified organic O-layers and 23 Ah-horizon soil samples) were collected (cf. Lemma et al. 2019 and Mekonnen et al. 2019).

Late Glacial and Holocene sediment samples were collected from the glacial lake Garba Guracha and a periodically dry depression referred to as "B4" (cf. Bittner et al. 2020 and Mekonnen et al. 2022, respectively). In brief, Garba Guracha is a NEE-oriented glacial cirque located at 3950 m asl (6.875781° N, 39.878075° E) between the Ericaceous and afro-alpine belts. It is about 500 m long and 300 m wide, has a maximum water depth of 6 m, and has a watershed of 0.15 km^2. Previous studies by Umer et al. (2007) and Tiercelin et al. (2008) provided a detailed description of the lake's geochemistry. In 2017, Bittner et al. (2020) retrieved a 15 m long core using a Livingstone piston corer operated from a raft anchored at 4.8 m of water depth. Sediments were sub-sampled in the laboratory from the core depth between 75 and 948 cm at 10 cm intervals for *n*-alkanes (n = 88) and sugar biomarker (n = 69) analyses. Further details on the core retrieval, stratigraphy, and chronology of this 16.7 kyr BP paleolimnological archive are presented in Bittner et al. (2020).

The B4 depression is located above the upper limit of the Ericaceous belt at 3970 m asl (6.88905° N; 39.90869° E). A pit profile with humic-rich lacustrine sediments was dug down to a depth of 2.55 m, and samples were taken every 2-cm, from 69 to 255 cm, and every 5 cm above 69 cm. In brief, the B4 profile is composed of three stratigraphic units covering the Late Glacial and Holocene according to Mekonnen et al. (2022). Unit 1 (255–175 cm) is dark-grey, laminated silty-clay above a thin grayish sandy silt layer and basalt boulders. Unit 2, from 175 to 70 cm depth, is gray partly laminated silty clay, deposited between 16.6 and 13.6 cal kyr BP. Unit 3 is about 70 cm thick and consists of light brown, weakly clayey sandy silt with red mottles and bleached aggregate surfaces, indicating waterlogging during the rainy season. Given that Unit 3 is strongly affected by degradation; only the 34 *n*-alkane data from Unit 1 and 2 were

further evaluated within this study here. The basal sediments of this profile are dated to 18 cal kyr BP.

Laboratory analyses

n-Alkane and sugar biomarker analyses

The analyses for all here reviewed *n*-alkane datasets (Lemma et al. 2019; Bittner et al. 2020; Mekonnen et al. 2022) were carried out using the Soxhlet lipid extraction method by adding dichloromethane (DCM) and methanol (MeOH) as solvents (9:1 ratio) for 24 h, following the method described by Zech and Glaser (2008). After obtaining the total lipid extracts (TLEs), 5α-androstane was added as an internal standard to the TLEs. The samples were concentrated using rotary evaporation and transferred to aminopropyl columns. The *n*-alkanes were eluted from the TLEs using 3 mL of hexane as solvent. Subsequently, the *n*-alkanes were quantified using a GC-2010 series gas chromatograph coupled with a flame ionization detector (GC-FID; Shimadzu, Kyoto, Japan). The GC instrument was equipped with an SPB-5 column (28.8 m length, 0.25 mm inner diameter, and 0.25 µm film thickness). An *n*-alkane mixture (C_8–C_{40}) was used as an external standard for linear calibration, and helium was used as a carrier gas.

The analyses for the reviewed sugar dataset from modern reference samples and the newly generated sugar dataset from Garba Guracha (B4 sediments were not studied using sugars) were carried out following the method described by Mekonnen et al. (2019). Samples were hydrolyzed at 105 °C for four hours after adding 10 ml of 4 M trifluoroacetic acid (TFA) and 100 µg of the internal recovery standard (myo-inositol). The hydrolyzed samples were filtrated over glass fiber filters, and TFA was removed using a rotary evaporator. The samples were further purified over XAD-7 and DOWEX 50WX8 columns. Thereafter, the sugars were freeze-dried and derivatized. Unlike Bittner et al. (2020), who applied methylboronic acid (MBA) derivatization, we used N-methyl-2-pyrrolidone (NMP) and N, O-Bis(trimethylsilyl) trifluoroacetamide (BSTFA) for derivatization following the procedure described by Mekonnen et al. (2019). This has the advantage that in addition to arabinose, fucose, and xylose, also fructose, galactose, glucose, mannose, rhamnose, and ribose can be quantified using subsequent gas chromatograph-flame ionization detection (GC-FID, Shimadzu, Kyoto, Japan). Still, glucose was not further considered during data evaluation because the partial contribution of cellulose structures could not be excluded. Similarly, fructose and ribose were not further evaluated because of their very low concentrations.
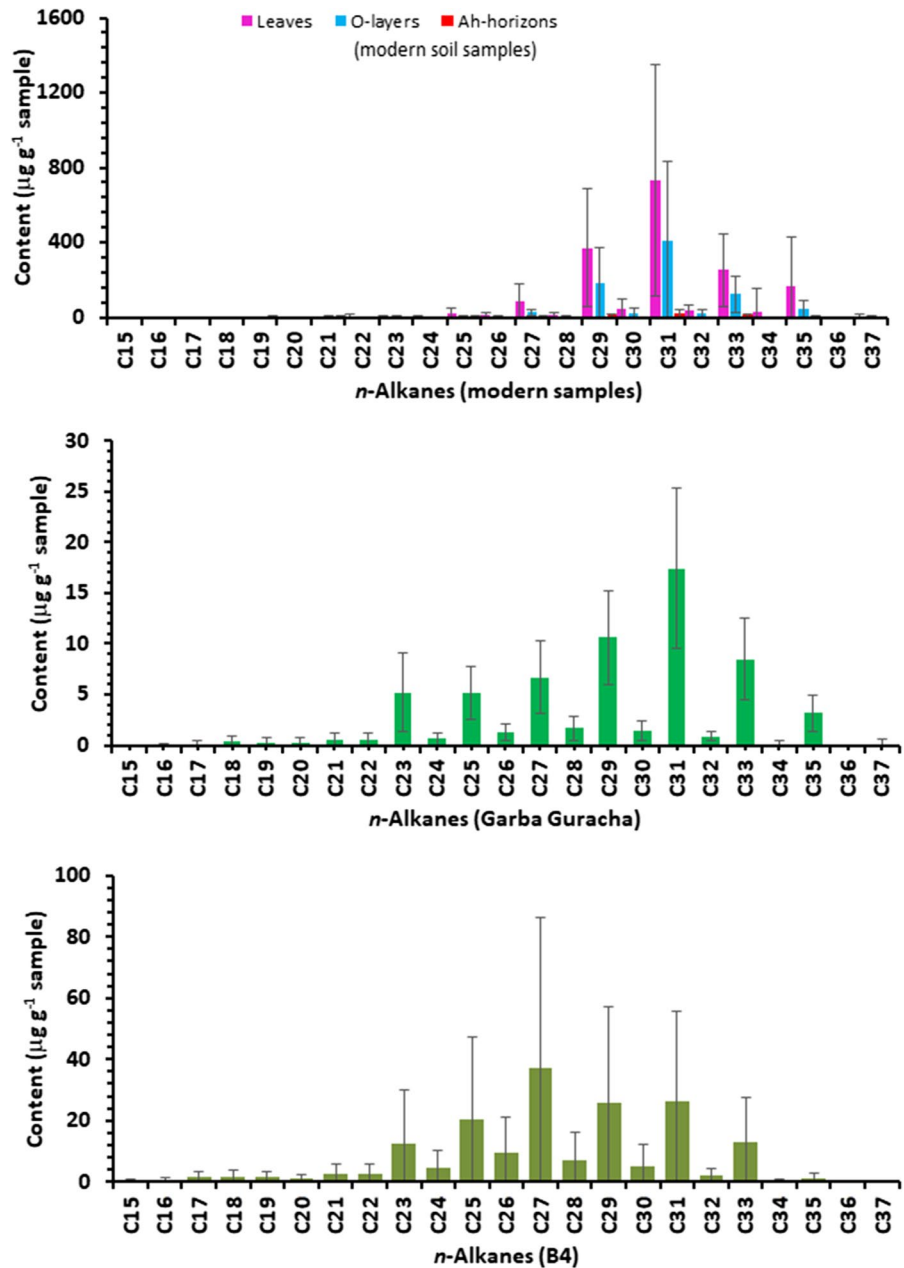
Results

n-Alkane contents and patterns of modern plants, top soils, and sediment samples

The average total *n*-alkane contents are 1764, 859, and 58 µg g^{-1} for leaves, O-layers, and Ah-horizons, respectively, according to the dataset published by Lemma et al. (2019) (Fig. 2). In the Garba Guracha and B4 sediments, the average total *n*-alkane contents are 64 and 177 µg g^{-1}, respectively, according to the datasets published by Bittner et al. (2020) and Mekonnen et al. (2022). All *n*-alkane patterns reveal a strong odd-over-even predominance (OEP). The long-chain *n*-alkanes C_{29}, C_{31}, and C_{33} are dominant in modern samples. While C_{31} is the predominant *n*-alkane also in the Garba Guracha sediments, C_{27} is predominant in the B4 sediments. In contrast to the modern samples, the mid-chain *n*-alkanes C_{23} and C_{25} are abundantly present in the sediment of B4 and Garba Guracha (Figs. 2 and 4).

The relative abundances of mid- and long-chain *n*-alkanes for all samples are presented in the form of ternary diagrams in Fig. 3. Accordingly, regarding the homologues C_{29}, $C_{31,}$ and C_{33} (Fig. 3a), the modern samples show a larger variability than the sediments of Garba Guracha and B4. Still, the mean relative abundances of these long-chain homologues are quite congruent. However, when the *n*-alkane homologue series $\leq C_{27}$ are included in the ternary diagrams, the congruency of the modern samples with the sedimentary samples disappears. For instance, with regard to the homologues C_{27}, $C_{29,}$ and C_{31}, most terrestrial samples are characterized by relative abundances of $C_{27} < 10\%$, whereas relative abundances of $C_{27} > 10\%$ are characteristic for the sediments of Garba Guracha and B4 (Fig. 3b). Similarly, including mid-chain homologues in the ternary diagrams reveals that the relative abundances of C_{25} and C_{23} are typically $< 10\%$ in most terrestrial samples. By contrast, the relative abundances of C_{25} and C_{23} are typically $> 10\%$ in the

Fig. 2 Average *n*-alkane contents and patterns of leaves, O-layers, and Ah-horizons (Lemma et al. 2019), as well as of the Garba Guracha and B4 sediments

sediments of Garba Guracha and B4 (Fig. 3c). Figure 4 depicts that modern samples (leaves, O-layers, and Ah-horizons) yielded P_{aq} values typically < 0.1, whereas the Garba Guracha and B4 sediments yielded P_{aq} values typically > 0.2.

Sugar contents and patterns of modern plants, top soils, and sediment samples.

The average sugar contents in the modern samples range between 0.8 (fucose in topsoils) and 40.7 mg g^{-1} (xylose in leaves), according to the dataset published by Mekonnen et al. (2019), whereas for the Garba Guracha sediment samples, they range between 2.3 (rhamnose) and 4.4 mg g^{-1} (galactose) (Fig. 5). No sugar analyses were carried out for the B4 sediments. The modern samples are characterized by a pronounced predominance of xylose, arabinose, and galactose, and all sugar biomarkers significantly decrease from the leaves to the Ah-horizons.
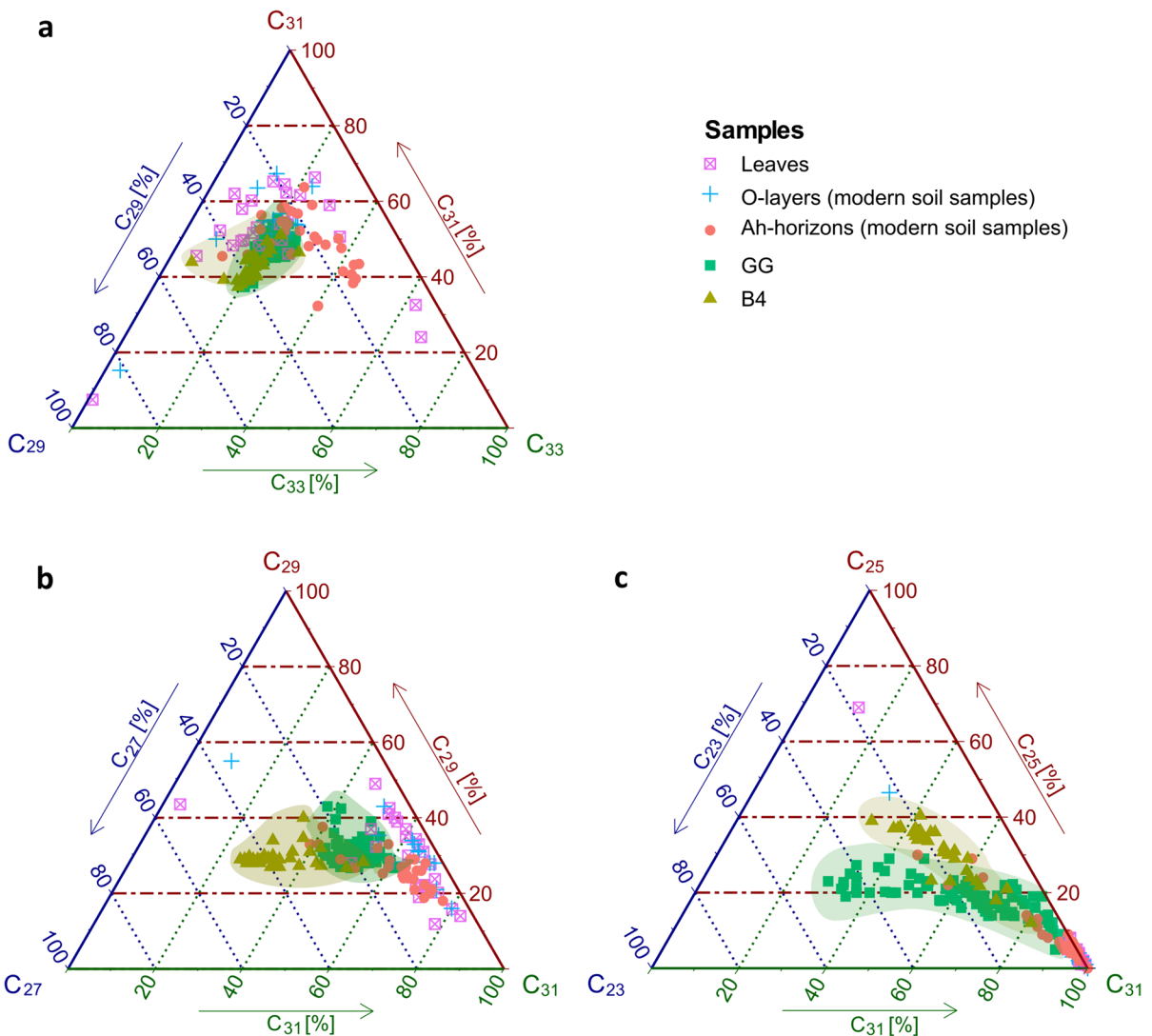
Fig. 3 Ternary diagrams for the relative abundances (%) of long- and mid-chain *n*-alkanes in modern leaf and soil samples (Lemma et al. 2019) versus in Garba Guracha and B4 sediment samples

By contrast, the predominance of xylose, arabinose, and galactose is by far less pronounced for the Garba Guracha sediments (Fig. 5).

Figure 6 depicts the relative abundances of the individual sugar biomarkers. Accordingly, xylose and galactose are the most abundant hemicellulose-derived sugar in leaves, followed by arabinose. The relative abundances of xylose, arabinose, and galactose significantly decrease from leaves over O-layers to the Ah-horizons (Fig. 6). By contrast, the relative abundance of mannose substantially increases. The relative abundances of rhamnose and fucose are very

low in leaves and do not show significant increases from leaves to the Ah-horizons (Fig. 6).

Galactose is the predominant sugar biomarker in the Garba Guracha sediments, followed by xylose, fucose, arabinose, mannose, and rhamnose. The relative abundances of fucose and rhamnose are significantly higher in the Garba Guracha sediments than in the modern samples (Fig. 6). Therefore, we calculated the ratio (fuc+rham)/(ara+xyl) as a proxy for organic matter source identification. Our comparison reveals significantly higher values for the Garba Guracha sediments than for the modern samples

Fig. 4 Comparison of the P_{aq} ratios yielded for leaves (n = 25), O-layers (n = 15), Ah-horizons (n = 23) versus sediments from B4 (n = 34) (Mekonnen et al. 2022) and Garba Guracha (n = 88) (Bittner et al. 2020). The notched box plots indicate the median (solid lines between the boxes) and interquartile range (IQR) with upper (75%) and lower (25%) quartiles. The notches display the 95% confidence interval of the median. The lines extending outside the box (whiskers) show variability outside the quartiles. The circles represent outliers
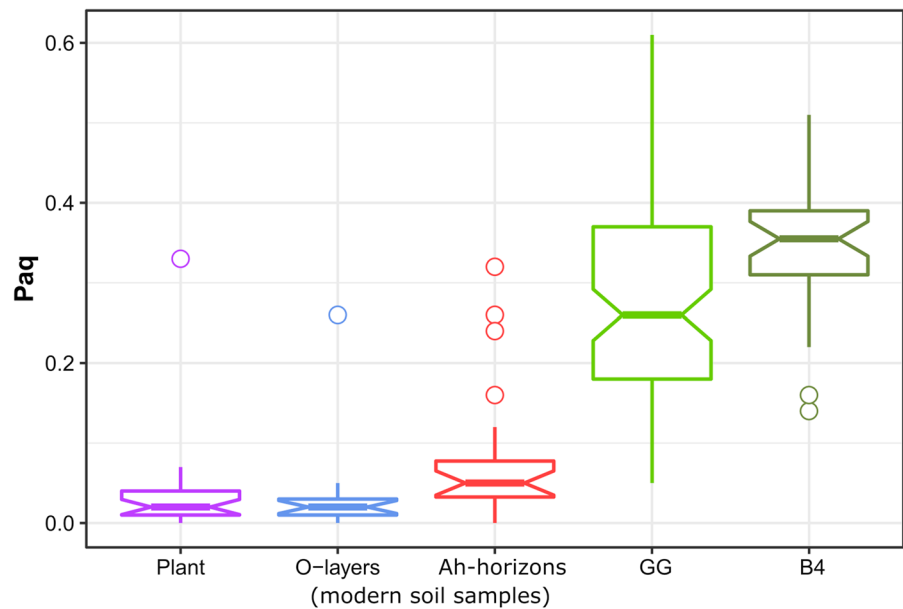
(Fig. 7). The sediments are typically characterized by (fuc + rham)/(ara + xyl) ratios > 0.75, whereas the modern leaf and soil samples are typically characterized by ratios < 0.75.

Discussion

Terrestrial versus aquatic source identification of the sedimentary n-alkanes

The dominance of long-chain *n*-alkanes in modern samples from the Sanetti Plateau is consistent with several studies reporting the dominance of long-chain *n*-alkanes in leaves and modern soils (Eglinton and Hamilton 1967; Bush and McInerney 2013). The low *n*-alkane contents in modern soils can be explained by dilution with minerogenic soil components as well as by degradation (Zech et al. 2011; Schäfer et al. 2016). The average total *n*-alkane content is higher in B4 than in Garba Guracha, likely due to high *n*-alkane preservation in the lower section of the profile.

As shown in Fig. 3a using a ternary diagram, the relative contributions of the sedimentary *n*-alkane homologues C_{29}, C_{31}, and C_{33} are well concordant with the modern leaves, O-layer, and Ah-topsoil samples. Albeit this is no prove, it indicates that these sedimentary long-chain *n*-alkanes are likely primarily of terrestrial (allochthonous) origin. By contrast,

the concordance in the ternary diagrams of Fig. 3 is lost when including the *n*-alkane homologues C_{23}, C_{25}, and C_{27}. This suggests that these sedimentary *n*-alkanes are not of pure terrestrial origin but at least partly originate from a different source. Indeed, Ficken et al. (2000) reported on aquatic macrophytes producing such homologues and proposed the P_{aq} ratio $(C_{23}+C_{25})/(C_{23}+C_{25}+C_{29}+C_{31})$ as a proxy to identify the sedimentary input of submerged or floating aquatic macrophytes. According to Ficken et al. (2000), P_{aq} values < 0.1 are characteristic for terrestrial plants, whereas values between 0.1 and 1 are characteristic for emergent and submerged macrophytes. This boundary is also well suited for distinguishing our modern reference (terrestrial) and sediment samples (Fig. 4) and, at the same time, strongly suggests that the sedimentary *n*-alkane homologues C_{23} and C_{25} in Garba Guracha and B4 are mainly aquatic-derived.

While Bittner et al. (2020) stated that an unambiguous terrestrial versus aquatic source identification of the *n*-alkane record of Garba Guracha seems challenging at the current state of research, the results and the interpretation of our comparative approach are well in agreement with other studies reporting on short- and mid-chain *n*-alkane production by submerged and floating plants, algae, and bacteria (e.g. Aichner et al. 2010; Cranwell et al. 1987; Liu and Liu 2016).

Fig. 5 Average contents of the sugar biomarkers xylose, arabinose, rhamnose, fucose, mannose, and galactose in leaves, O-layers, Ah-horizons (Mekonnen et al. 2019) and the Garba Guracha sediments
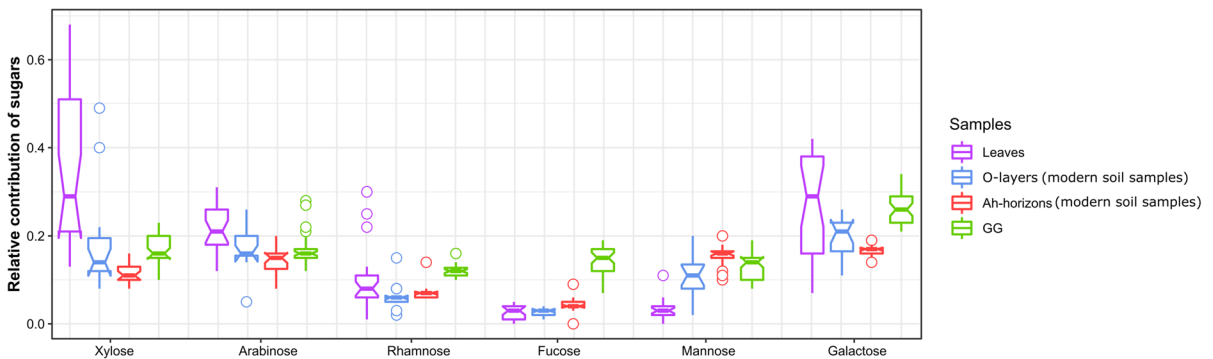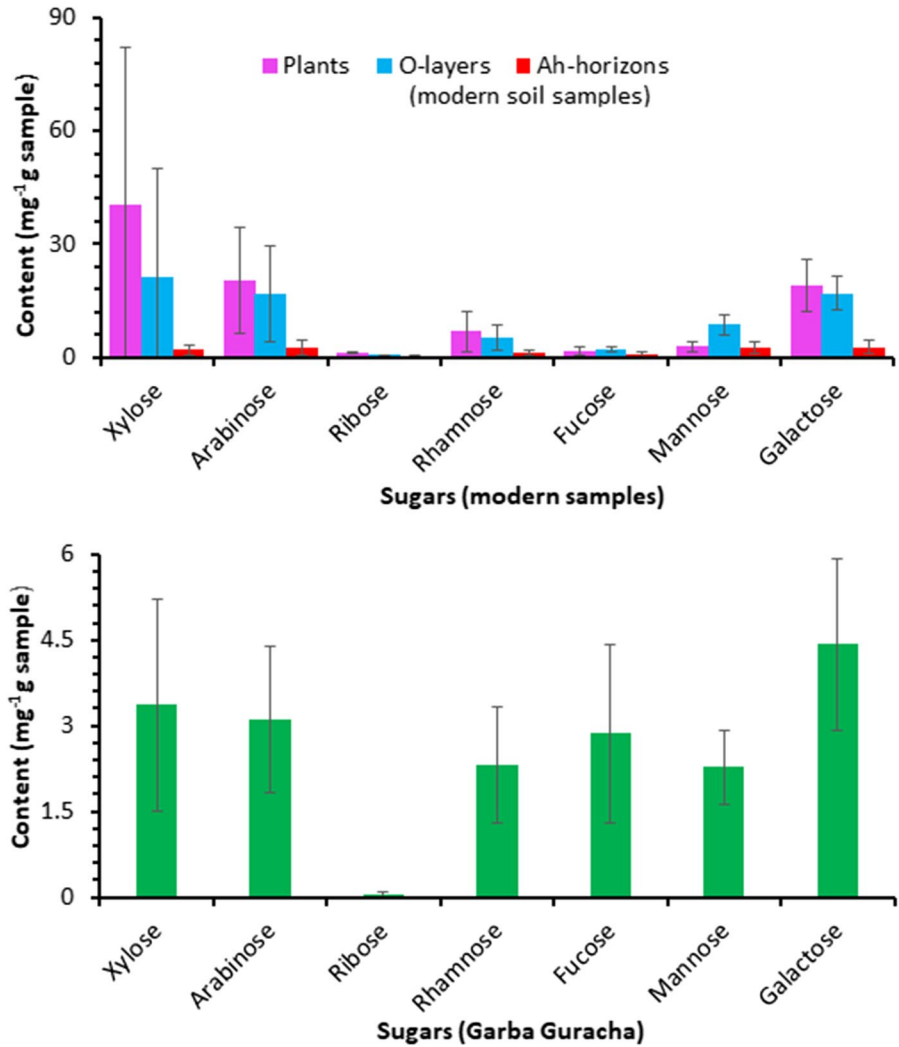

Fig. 6 Relative abundances of sugar biomarkers in leaves (n = 25), O-layers (n = 15), Ah-horizons (n = 23) and the Garba Guracha sediments (n = 69). The notched box plots indicate the median (solid lines between the boxes) and interquartile range (IQR) with upper (75%) and lower (25%) quartiles. The notches display the 95% confidence interval of the median. The lines extending outside the box (whiskers) show variability outside the quartiles. The circles represent outliers

Fig. 7 The ratio (fuc + rham)/(ara + xyl) in leaves (n = 25), O-layers (n = 15), Ah-horizons (n = 23), and the Garba Guracha sediments (n = 69). The notched box plots indicate the median (solid lines between the boxes) and interquartile range (IQR) with upper (75%) and lower (25%) quartiles. The notches display the 95% confidence interval of the median. The lines extending outside the box (whiskers) show variability outside the quartiles. The circles represent outliers
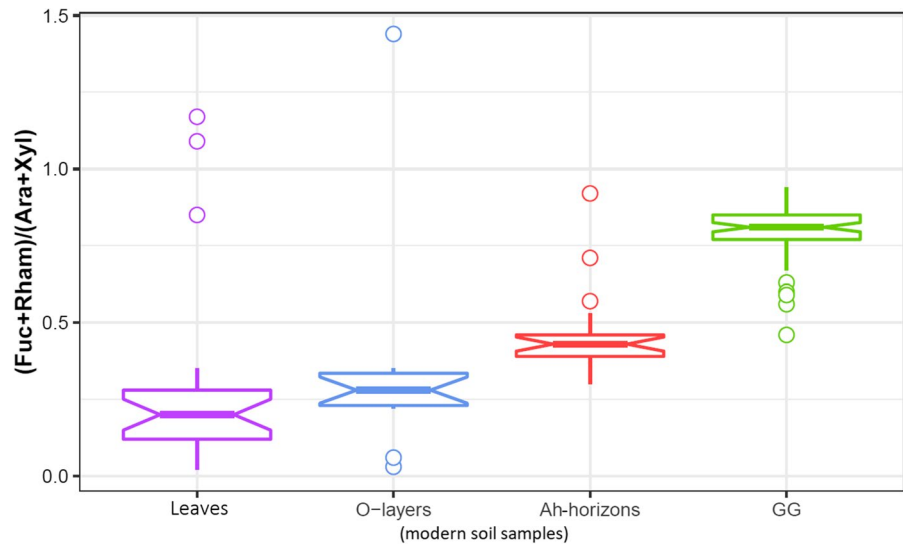
Still, it is noteworthy that the interpretation of the sedimentary long-chain homologues in terms of primarily terrestrial input is not completely unambiguous. According to Lichtfouse et al. (1994), Dennis and Kolattukudy (1991), Metzger and Largeau (2005) and He et al. (2018), *Botryococcus braunii*, a green algae commonly found in tropical freshwater lakes (Jankovská and Komárek 2000), is characterized by an abundant production of the long-chain n-alka-dienes C_{27}, C_{29}, and C_{31}. A diagenetic reduction is suggested as an important source of sedimentary n-alkanes. Indeed, Umer et al. (2007) found abundant *Botryococcus* pollen in the Garba Guracha sediments. Similarly, pollen results from the B4 sediments show high amounts of *Botryococcus*, especially at the bottom of the profile (Mekonnen et al. 2022). Therefore, *Botryococcus* may not be excluded from having also contributed to the long-chain n-alkanes of the sedimentary archives of the Bale Mountains. According to published data, the ambiguity in the interpretation of sedimentary long-chain n-alkanes can be alleviated by compound specific δ13C values of the n-alkanes and through the application of isotopic mixing models (Aichner et al., 2010; Gao et al., 2011; Liu et al., 2015; Andrae et al., 2020; Yang and Bowen, 2022). Andrae et al. (2020) for instance have shown that in their case study from Australia aquatic macrophyte input significantly influenced the δ13C isotopic composition of the long-chain n-alkanes C27 and C29. This finding together with our own results shown in Figs. 2 and 3b suggests that the C27 n-alkane

homologue in the Garba Guracha and B4 sediments are the results of mixing terrestrial and aquatic sources. While bulk δ13C values for Garba Guracha (ranging between -22.7 and -13.9 ‰) and B4 (average ~ 14 ‰) clearly indicate that bulk sedimentary organic matter is strongly influenced by aquatic input, compound-specific δ13C analyses were only realized on two selected samples from B4 for the most abundant long-chain n-alkanes C27, C29 and C31 (Mekonnen et al., 2022). The obtained δ13Cn-alkane values range from -22.1 to -29.8‰ and hence reflect an isotopic mixing of aquatic and terrestrial sources for these long-chain n-alkanes.

Last but not least, apart from "terrestrial" versus "aquatic" input, a "microbial" input should not be completely overlooked. Several studies have highlighted that soil micro-organisms (as well as likely sedimentary micro-organisms) do not only degrade organic matter, including n-alkanes, but are also able to contribute to the built-up of a microbial short-, mid-, and even long-chain n-alkane pool in soils and sediments (Jones 1969; Nguyen Tu et al. 2011; Zech et al. 2011; Brittingham et al. 2017; Li et al. 2018).

Terrestrial versus aquatic source identification of the sedimentary sugar biomarkers

As presented above, the leaf samples from the San-etti Plateau are characterized by high abundances of xylose and arabinose. This is in agreement with literature reporting on the high production of these

sugar biomarkers by vascular plants (Oades 1984; Jia et al. 2008; Hepp et al. 2016). Similarly, the high abundance of galactose in the terrestrial reference dataset of Mekonnen et al. (2019) is well explicable with dominant vegetation such as *Erica*, *Alchemilla*, and *Lobelia* (Schädel et al. 2010; Gunina and Kuzyakov 2015). The significant decrease of most sugars from leaves to soils can be attributed to dilution with minerogenic soil components as well as to degradation (Hedges et al. 1985; Jia et al. 2008). For instance, Jia et al. (2008) and Hernes et al. (1996) reported on the labile nature of arabinose and glucose, whereas fucose, rhamnose, xylose, and mannose were described as more refractory. In the terrestrial reference dataset of Mekonnen et al. (2019), mannose is the only sugar substantially increasing with regard to its relative contribution in soils. This likely reflects the soil microbial build-up of this sugar biomarker. Indeed, Oades (1984) and Murayama (1984) reported on the substantial synthesis of mannose by soil microbial populations. The dataset of Mekonnen et al. (2019) does not show a significant increase in the relative abundances of rhamnose and fucose from the leaf to the soil samples. This contrasts with studies showing such an increase during soil degradation (Murayama 1984; Oades 1984).

Given the high terrestrial production of xylose and arabinose (Fig. 5), we suggest that their predominance in the Garba Guracha sediments reflects an at least partly terrestrial input. The relatively high abundances of galactose and mannose in the Garba Guracha sediments might be attributed to contributions by both soil and aquatic micro-organisms. According to Oades (1984), the ratio (G + M)/(A + X) can serve as a proxy to differentiate between plant-derived and microbial-derived sugars in soils. However, because galactose and mannose are produced by both soil and aquatic bacteria, their use for identifying terrestrial versus aquatic input is challenging. The results of our comparative approach show that the relative contributions of rhamnose and fucose are significantly higher in sediments compared to the terrestrial reference samples of Mekonnen et al. (2019) (Fig. 6). Rhamnose and fucose are reported to occur in submerged aquatic plants (Jia et al. 2008). Furthermore, organic matter decomposition in sediments can lead to the in situ microbial synthesis of fucose and rhamnose (Marchand et al. 2005). Last but not least, also Hepp et al. (2016) reported that fucose is abundantly produced by algae and zooplankton, whereas xylose and arabinose strongly predominate in terrestrial plants and soils. This different behavior of the here discussed specific sugar biomarkers results in the ratio of (fuc + rham)/(ara + xyl) clearly allowing to distinguish between modern terrestrial reference samples of Mekonnen et al. (2019) and Garba Guracha sediments (Fig. 7). This finding suggests that the ratio (fuc + rham)/(ara + xyl) is a promising proxy for terrestrial versus aquatic source identification, also beyond our case study.

Conclusions

In this study, we aimed to identify the terrestrial versus aquatic sources of partly published *n*-alkane and sugar biomarker datasets from two afro-alpine sedimentary archives in the Bale Mountains of Ethiopia. We compared the Late Glacial and Holocene sedimentary biomarker patterns with those of published modern plants and soils serving as terrestrial reference samples. Our comparative approach shows that long-chain *n*-alkanes predominate in both the modern and sediment samples. Ternary diagrams reveal that there is a high concordance of the sedimentary C_{29}, C_{31}, and C_{33} patterns with those of the terrestrial samples, whereas C_{23}, C_{25}, and C_{27} occur at strikingly higher relative abundances in the sediments. This strongly indicates that the latter are produced by aquatic macrophytes and micro-organisms. The P_{aq} ratio $(C_{23} + C_{25})/(C_{23} + C_{25} + C_{29} + C_{31})$ reveals a significant difference between modern plant and soil samples and the sediments. Regarding the sugar biomarkers, unambiguous terrestrial versus aquatic source identification of arabinose and xylose in the sediments is challenging. By contrast, the much higher relative abundances of rhamnose and fucose in the sediments compared to modern plants and soils corroborate that they are mainly produced by aquatic macrophytes and micro-organisms. Therefore, we propose that the ratio (fuc + rham)/(ara + xyl) is a valuable sugar biomarker proxy for distinguishing aquatic versus terrestrial origin. The last conclusion that can be drawn from our comparative approach is that no unambiguous source identification is possible for sedimentary galactose and mannose.

Declarations

Conflict of interest The authors declare no competing interests.

References

Aichner B, Herzschuh U, Wilkes H (2010) Influence of aquatic macrophytes on the stable carbon isotopic signatures of sedimentary organic matter in lakes on the Tibetan Plateau. Org Geochem 41:706–718. https://doi.org/10.1016/j.orggeochem.2010.02.002

Andersson RA, Meyers P, Hornibrook E et al (2012) Elemental and isotopic carbon and nitrogen records of organic matter accumulation in a holocene permafrost peat sequence in the east european russian arctic. J Quat Sci 27:545–552. https://doi.org/10.1002/jqs.2541

Andrae JW, McInerney FA, Sniderman JMK (2020) Carbon isotope systematics of leaf wax n-alkanes in a temperate lacustrine depositional environment. Org Geochem 150:104121. https://doi.org/10.1016/j.orggeochem.2020.104121

Billi P (2015) Geomorphological Landscapes of Ethiopia. In: Billi P (ed) Landscapes and landforms of Ethiopia. Springer Netherlands, Dordrecht, pp 3–32

Bittner L, Bliedtner M, Grady D et al (2020) Revisiting afro-alpine Lake Garba Guracha in the Bale Mountains of Ethiopia: rationale, chronology, geochemistry, and paleoenvironmental implications. J Paleolimnol. https://doi.org/10.1007/s10933-020-00138-w

Brittingham A, Hren MT, Hartman G (2017) Microbial alteration of the hydrogen and carbon isotopic composition of n-alkanes in sediments. Org Geochem 107:1–8. https://doi.org/10.1016/j.orggeochem.2017.01.010

Bush RT, McInerney FA (2013) Leaf wax n-alkane distributions in and across modern plants: implications for paleoecology and chemotaxonomy. Geochim Cosmochim Acta 117:161–179. https://doi.org/10.1016/j.gca.2013.04.016

Cheshire MV (1979) Nature and origin of carbohydrates in soil. Academic Press, London, p 216

Chignell SM, Laituri MJ, Young NE, Evangelista PH (2019) Afroalpine wetlands of the Bale Mountains, Ethiopia: distribution, dynamics, and conceptual flow model. Annals American Assoc Geog 109:791–811

Cranwell PA, Eglinton G, Robinson N (1987) Lipids of aquatic organisms as potential contributors to lacustrine sediments-II. Org Geochem 11:513–527. https://doi.org/10.1016/0146-6380(87)90007-6

Dennis MW, Kolattukudy PE (1991) Alkane biosynthesis by decarbonylation of aldehyde catalyzed by a microsomal preparation from Botryococcus braunii. Arch Biochem Biophys 287:268–275. https://doi.org/10.1016/0003-9861(91)90478-2

Doyle RM, Longstaffe FJ, Moser KA (2022) An isotope, elemental, and n-alkane baseline for organic matter sources in sediments of high-altitude lakes in the Uinta Mountains, Utah, USA. J Paleolimnol 69:123–139. https://doi.org/10.1007/s10933-022-00265-6

Dullo BW, Grootjans AP, Roelofs JGM et al (2015) Fen mires with cushion plants in Bale Mountains, Ethiopia. Mires Peat 15:1–10

Eglinton G, Hamilton RJ (1967) Leaf epicuticular waxes. Sci (80-) 156:1322–1335. https://doi.org/10.1126/science.156.3780.1322

Ficken KJ, Li B, Swain DL, Eglinton G (2000) An n-alkane proxy for the sedimentary input of submerged/floating freshwater aquatic macrophytes. Org Geochem 31:745–749. https://doi.org/10.1038/nmat4240

Ficken KJ, Wooller MJ, Swain DL et al (2002) Reconstruction of a subalpine grass-dominated ecosystem, Lake Rutundu, Mount Kenya: a novel multi-proxy approach. Palaeogeogr Palaeoclimatol Palaeoecol 177:137–149. https://doi.org/10.1016/S0031-0182(01)00356-X

Friis I (1986) Zonation of forest vegetation on the South Slope of Bale Mountains, South Ethiopia. SINET Ethiop J Sci 9:29–44

Gao L, Hou J, Toney J, MacDonald D, Huang Y (2011) Mathematical modeling of the aquatic macrophyte inputs of mid-chain n-alkyl lipids to lake sediments: Implications for interpreting compound specific hydrogen isotopic records. Geochimica et Cosmochimica Acta 75(13):3781–3791

Gil-Romera G, Adolf C, Benito BM et al (2019) Long-term fire resilience of the Ericaceous Belt, Bale Mountains, Ethiopia. Biol Lett 15:20190357. https://doi.org/10.1098/rsbl.2019.0357

Groos AR, Akçar N, Yesilyurt S, Miehe G (2021) Nonuniform late pleistocene glacier fluctuations in tropical Eastern Africa. Sci Adv. https://doi.org/10.1126/sciadv.abb6826

Gunina A, Kuzyakov Y (2015) Soil biology & biochemistry sugars in soil and sweets for microorganisms: review of origin, content, composition and fate. Soil Biol Biochem 90:87–100

He D, Simoneit BRT, Jaffé R (2018) Environmental factors controlling the distributions of Botryococcus braunii (A, B and L) biomarkers in a subtropical freshwater wetland. Sci Rep 8:1–9. https://doi.org/10.1038/s41598-018-26900-9

Hedberg O (1951) Vegetation belts of the east african mountains, 45th edn. Sven. Bot. Tidskr, Stockholm

Hedberg O (1964) Features of afroalpine plant ecology. Swedish Science Press, Uppsala, Sweden

Hedges JI, Cowie GL, Ertel JR et al (1985) Degradation of carbohydrates and lignins in buried woods. Geochim Cosmochim Acta 49:701–711. https://doi.org/10.1016/0016-7037(85)90165-6

Hepp J, Rabus M, Anhäuser T et al (2016) A sugar biomarker proxy for assessing terrestrial versus aquatic sedimentary input. Org Geochem 98:98–104. https://doi.org/10.1016/j.orggeochem.2016.05.012

Hernes PJ, Hedges JI, Peterson ML et al (1996) Neutral carbohydrate geochemistry of particulate material in the central equatorial Pacific. Deep Res Part II Top Stud Oceanogr 43:1181–1204. https://doi.org/10.1016/0967-0645(96)00012-4

Hillman JC (1988) The Bale Mountains National Park Area, Southeast Ethiopia, and its management. Mt Res Dev 8:253–258

Jankovská V, Komárek J (2000) Indicative value of Pediastrum and other coccal green algae in palaeoecology. Folia Geobot 35:59–82. https://doi.org/10.1007/BF02803087

Jia G, Dungait JAJ, Bingham EM et al (2008) Neutral monosaccharides as biomarker proxies for bog-forming plants for application to palaeovegetation reconstruction in ombrotrophic peat deposits. Org Geochem 39:1790–1799. https://doi.org/10.1016/j.orggeochem.2008.07.002

Jones JG (1969) Studies on lipids of soil micro-organisms with particular reference to hydrocarbons. J Gen Microbiol 59:145–152. https://doi.org/10.1099/00221287-59-2-145

Kidane Y, Stahlmann R, Beierkuhnlein C (2012) Vegetation dynamics, and land use and land cover change in the Bale Mountains, Ethiopia. Environ Monit Assess 184:7473–7489. https://doi.org/10.1007/s10661-011-2514-8

Kuzmicheva EA, Khasanov BF, Krylovich OA, Savinetsky AB (2014) Vegetation and climate reconstruction for the bale mountains (Ethiopia) in the Holocene according to the pollen analysis and radiocarbon dating of zoogenic deposits. Dokl Biol Sci 458:281–285. https://doi.org/10.1134/S0012496614050019

Lemma B, Mekonnen B, Glaser B et al (2019) Chemotaxonomic patterns of vegetation and soils along altitudinal transects of the Bale Mountains, Ethiopia, and implications for paleovegetation reconstructions–part II: lignin-derived phenols and leaf-wax-derived n-alkanes. E&G Quat Sci J 68:189–200. https://doi.org/10.5194/egqsj-68-189-2019

Lemma B, Kebede Gurmessa S, Nemomissa S et al (2020) Spatial and temporal 2H and 18O isotope variation of contemporary precipitation in the Bale Mountains, Ethiopia. Isot Environ Health Stud 56:122–135. https://doi.org/10.1080/10256016.2020.1717487

Li G, Li L, Tarozo R et al (2018) Microbial production of long-chain n-alkanes: implication for interpreting sedimentary leaf wax signals. Org Geochem 115:24–31. https://doi.org/10.1016/j.orggeochem.2017.10.005

Lichtfouse É, Derenne S, Mariotti A, Largeau C (1994) Possible algal origin of long chain odd n-alkanes in immature sediments as revealed by distributions and carbon isotope ratios. Org Geochem 22:1023–1027. https://doi.org/10.1016/0146-6380(94)90035-3

Liu H, Liu W (2016) n-Alkane distributions and concentrations in algae, submerged plants and terrestrial plants from the Qinghai-Tibetan Plateau. Org Geochem 99:10–22. https://doi.org/10.1016/j.orggeochem.2016.06.003

Liu W, Yang H, Wang H, An, Z, Wang Z, Leng Q (2015) Carbon isotope composition of long chain leaf wax n-alkanes in lake sediments: A dual indicator of paleoenvironment in the Qinghai-Tibet Plateau. Org Geochem 83–84:190–201. https://doi.org/10.1016/j.orggeochem.2015.03.017

Lüniger G, Schwark L (2002) Characterisation of sedimentary organic matter by bulk and molecular geochemical proxies: an example from oligocene maar-type Lake Enspel, Germany. Sediment Geol 148:275–288. https://doi.org/10.1016/S0037-0738(01)00222-6

Marchand C, Disnar JR, Lallier-Vergés E, Lottier N (2005) Early diagenesis of carbohydrates and lignin in mangrove sediments subject to variable redox conditions (french Guiana). Geochim Cosmochim Acta 69:131–142. https://doi.org/10.1016/j.gca.2004.06.016

Mekonnen B, Zech W, Glaser B et al (2019) Chemotaxonomic patterns of vegetation and soils along altitudinal transects of the Bale Mountains, Ethiopia, and implications for paleovegetation reconstructions–part I: stable isotopes and sugar biomarkers. E&G Quat Sci J 68:177–188. https://doi.org/10.5194/egqsj-68-177-2019

Mekonnen B, Glaser B, Zech R et al (2022) Climate, vegetation and fire history during the past 18,000 years, recorded in high altitude lacustrine sediments on the Sanetti Plateau, Bale Mountains (Ethiopia). Prog Earth Planet Sci. https://doi.org/10.1186/s40645-022-00472-9

Metzger P, Largeau C (2005) Botryococcus braunii: a rich source for hydrocarbons and related ether lipids. Appl Microbiol Biotechnol 66:486–496. https://doi.org/10.1007/s00253-004-1779-z

Meyers PA (1994) Preservation of elemental and isotopic source identification of sedimentary organic matter.

Chem Geol 114:289–302. https://doi.org/10.1016/0009-2541(94)90059-0

Meyers PA, Ishiwatari R (1993) Lacustrine organic geochemistry-an overview of indicators of organic matter sources and diagenesis in lake sediments. Org Geochem 20:867–900. https://doi.org/10.1016/0146-6380(93)90100-P

Meyers PA, Lallier-Vergès E (1999) Lacustrine sedimentary organic matter records of late quaternary paleoclimates. J Paleolimnol 21:345–372. https://doi.org/10.1023/A:1008073732192

Miehe G, Miehe S (1994) Ericaceous forests and heathlands in the Bale Mountains of South Ethiopia: ecology and man's impact. T. Warnke Verlag, Hamburg, Germany

Murayama S (1984) Changes in the monosaccharide composition during the decomposition of straws under field conditions. Soil Sci Plant Nutr 30:367–381. https://doi.org/10.1080/00380768.1984.10434702

Nguyen Tu TT, Egasse C, Zeller B et al (2011) Early degradation of plant alkanes in soils: a litterbag experiment using 13 C-labelled leaves. Soil Biol Biochem 43:2222–2228. https://doi.org/10.1016/j.soilbio.2011.07.009

Oades JM (1984) Soil organic matter and structural stability: mechanisms and implications for management. Plant Soil 76:319–337. https://doi.org/10.1007/BF02205590

Osmaston HA, Mitchell WA, Osmaston JAN (2005) Quaternary glaciation of the Bale Mountains, Ethiopia. J Quat Sci. https://doi.org/10.1002/jqs.931

Ossendorf G, Groos AR, Bromm T et al (2019) Middle Stone Age foragers resided in high elevations of the glaciated Bale Mountains, Ethiopia. Sci (80-) 365:583–587. https://doi.org/10.1126/science.aaw8942

Schädel C, Blöchl A, Richter A, Hoch G (2010) Quantification and monosaccharide composition of hemicelluloses from different plant functional types. Plant Physiol Biochem 48:1–8. https://doi.org/10.1016/j.plaphy.2009.09.008

Schäfer IK, Lanny V, Franke J et al (2016) Leaf waxes in litter and topsoils along a european transect. Soil 2:551–564. https://doi.org/10.5194/soil-2-551-2016

Smol JP, Birks HJB, Last WM (eds) (2002) Tracking Environmental Change using Lake sediments. Volume 3: Terrestrial, Algal, and Siliceous indicators. Kluwer Academic Publisher

Talbot MR, Livingstone DA (1989) Hydrogen index and carbon isotopes of lacustrine organic matter as lake level indicators. Palaeogeogr Palaeoclimatol Palaeoecol 70:121–137

Tiercelin JJ, Gibert E, Umer M et al (2008) High-resolution sedimentary record of the last deglaciation from a high-altitude lake in Ethiopia. Quat Sci Rev 27:449–467. https://doi.org/10.1016/j.quascirev.2007.11.002

Tierney JE, Smerdon JE, Anchukaitis KJ, Seager R (2013) Multidecadal variability in east african hydroclimate controlled by the Indian Ocean. Nature 493:389–392. https://doi.org/10.1038/nature11785

Umer M, Lamb HF, Bonnefille R et al (2007) Late pleistocene and holocene vegetation history of the Bale Mountains, Ethiopia. Quat Sci Rev 26:2229–2246. https://doi.org/10.1016/j.quascirev.2007.05.004

Wesche K, Miehe G, Kaeppeli M (2000) The significance of fire for Afroalpine Ericaceous Vegetation. Mt Res Dev 20:340–347. https://doi.org/10.1659/0276-4741(2000)020[0340:TSOFFA]2.0.CO;2

Woldu Z, Feoli E, Nigatu L (1989) Partitioning an elevation gradient of vegetation from southeastern Ethiopia by probabilistic methods. Vegetatio 81:189–198. https://doi.org/10.1007/BF00045524

Yang D, Bowen GJ (2022) Integrating plant wax abundance and isotopes for paleo-vegetation and paleoclimate reconstructions: a multi-source mixing model using a bayesian framework. Clim Past 18:2181–2210. https://doi.org/10.5194/cp-18-2181-2022

Yimer F (2007) Soil Properties in Relation to Topographic aspects. Vegetation Communities and Land Use in the South-eastern Highlands of Ethiopia

Yineger H, Kelbessa E, Bekele T, Lulekal E (2008) Floristic composition and structure of the Dry Afromontane Forest at Bale Mountains National Park, Ethiopia. J Sci 31:103–120. https://doi.org/10.4314/sinet.v31i2.66551

Zech M, Glaser B (2008) Improved compound-specific d13C analysis of n-alkanes for application in palaeoenvironmental studies. RAPID Commun MASS Spectrom 22:135–142. https://doi.org/10.1002/rcm.3342

Zech M, Pedentchouk N, Buggle B et al (2011) Effect of leaf litter degradation and seasonality on D/H isotope ratios of n-alkane biomarkers. Geochim Cosmochim Acta 75:4917–4928. https://doi.org/10.1016/j.gca.2011.06.006